Dynamic m6A mRNA methylation reveals the involvement of AcALKBH10 in ripening-related quality regulation in kiwifruit

New Phytologist

Dynamic m6A mRNA methylation reveals the involvement of AcALKBH10 in ripening-related quality regulation in kiwifruit

Journal:	*New Phytologist*
Manuscript ID	NPH-MS-2024-47578.R1
Manuscript Type:	Full Paper
Date Submitted by the Author:	10-Jul-2024
Key Words:	m6A RNA modification, kiwifruit ripening, fruit quality, AcALKBH10, AcECT9
Suggested Handling Editor:	

Complete List of Authors:
Liu, Mingchun; Sichuan University, College of Life Sciences
Su, Dan; Sichuan University, College of Life Sciences
Shu, Peng; Sichuan University, College of Life Sciences
Hu, Nan; Anyang Institute of Technology, College of Biology and Food Engineering
Chen, Yuan; Sichuan University, College of Life Sciences
Wu, Yi; Sichuan University, College of Life Sciences
Deng, Heng; Sichuan University, College of Life Science
Du, Xiaofei; Sichuan University, College of Life Sciences
Zhang, Xumeng; Sichuan University, College of Life Sciences
Wang, Ruochen; Sichuan University, College of Life Sciences
Li, Huajia; Sichuan Academy of Agricultural Sciences, Institute of Agro-Products Processing Science and Technology
Zeng, Yunliu; Huazhong Agriculture University, college of Horticulture & Forestry
Li, Da-wei; Chinese Academy of Sciences Wuhan Branch, Wuhan Botanical Garden,Chinese Academy of Sciences
Xie, Yue; Sichuan Provincial Academy of Natural Resource Sciences, Key Laboratory of Breeding and Utilization of Kiwifruit in Sichuan Province
Li, Mingzhang; Sichuan Academy of Natural Resource Sciences, Kiwifruit Breeding and Utilization Key Laboratory of Sichuan Province
Hong, Yiguo; University of Worcester, School of Science and the Environment
Liu, Kaidong; Lingnan Normal University, Life Science and Technology School

Data Availability Statement

Our Mandates Data Policy requires data to be shared and a Data Availability Statement, so please enter one in the space below. Sample statements can be found here. Please note that this statement will be published alongside your manuscript, if it is accepted for publication.

Data availability

The MeRIP sequencing datasets have been deposited in the Genome Sequence Archive at the National Genomics Data Center, Beijing Institute of Genomics, Chinese Academy of Sciences (http://bigd.big.ac.cn). The assigned accession number for the datasets is CRA011218, and they are accessible to the public.

Dynamic m6A mRNA methylation reveals the involvement of AcALKBH10 in ripening-related quality regulation in kiwifruit

Dan Su[1#], Peng Shu[1,3#], Nan Hu[4#], Yuan Chen[1], Yi Wu[1], Heng Deng[1], Xiaofei Du[1], Xumeng Zhang[1], Ruochen Wang[1], Huajia Li[5], Yunliu Zeng[6], Dawei Li[7], Yue Xie[8], Mingzhang Li[8*], Yiguo Hong[9,10], Kaidong Liu[2*], Mingchun Liu[1*]

[1]Key Laboratory of Bio-resource and Eco-environment of Ministry of Education, College of Life Sciences, Sichuan University, Chengdu, 610065, Sichuan, China

[2]Life Science and Technology School, Lingnan Normal University, Zhanjiang, 524048, China

[3]Clinical Medical Research Center, Xinqiao Hospital, Army Medical University, Chongqing, China

[4]College of Biology and Food Engineering, Anyang Institute of Technology, Anyang 455000, Henan, China

[5]Institute of Agro-Products Processing Science and Technology, Sichuan Academy of Agricultural Sciences, Chengdu 610066, China

[6]National Key Laboratory for Germplasm Innovation & Utilization of Horticultural Crops, College of Horticulture and Forestry Science, Huazhong Agricultural University, Wuhan, P.R. China

[7]Wuhan Botanical Garden, Chinese Academy of Sciences, Jiufeng 1 Road, Wuhan 430074, Hubei, China

[8]China-New Zealand the Belt and Road Joint Laboratory on Kiwifruit, Kiwifruit Breeding and Utilization Key Laboratory of Sichuan Province, Sichuan Academy of Natural Resource Sciences, Chengdu,610041, China

[9]School of Science and the Environment, University of Worcester, Worcester WR2 6AJ, UK

[10]State Key Laboratory of North China Crop Improvement and Regulation, College of Horticulture, Hebei Agricultural University, Baoding 071000, China

[#] These authors contributed equally.

[*]Correspondence should be addressed to: Mingchun Liu (mcliu@scu.edu.cn), Kaidong Liu (liukaidong2001@126.com), and Mingzhang Li (limzhang@163.com)

Summary

- Fruit ripening is a complex and highly coordinated process that occurs in conjunction with the formation of fruit edible quality. While genetic regulation has been a primary focus in previous research, the significance of epigenetic changes, particularly the impact of m6A RNA modification on fruit ripening and quality formation, has been largely overlooked.

- In this study, we monitored m6A level and its dynamic changes at four distinct development and ripening stages of kiwifruits. Notable m6A modifications occurred predominantly at the stop codons and the 3' UTRs and exhibited a gradual reduction in m6A levels during fruit ripening process. Moreover, these m6A modifications in the aforementioned sites demonstrated a discernible inverse relationship with the levels of mRNA abundance throughout ripening process, suggesting a repression effect of m6A modification in modulation of kiwifruit ripening.

- We further demonstrated that AcALKBH10 rather than AcECT9 predominantly regulates m6A levels in ripening-related genes, thereby exerting the regulatory control over the ripening process and the accumulation of soluble sugars and organic acids, ultimately influencing fruit ripening and quality formation. In conclusion, our findings illuminate the epi-regulatory mechanism involving m6A in kiwifruit ripening, offering a fresh perspective for cultivating high-quality kiwifruit with enhanced nutritional attributes.

Keywords: AcALKBH10, AcECT9, fruit quality, kiwifruit ripening, m6A RNA modification

Introduction

N6-methyladenosine (m6A) methylation is a prevalent mRNA modification found in eukaryotes, including plants. It involves the transfer of a methyl group to the N6 position of adenosines within mRNA molecules. This reversible modification is dynamically regulated by a complex interplay of "writers", "erasers" and "readers", which are enzymes and proteins responsible for m6A deposition, removal, and recognition, respectively (Huang et al., 2021; Yue et al., 2019; Zheng et al., 2020). The writers, such as METTL3 and METTL14, recognize specific RNA motifs and catalyze the transfer of a methyl group from S-adenosyl methionine (SAM) to mRNA (Arribas-Hernández and Brodersen, 2020; Bokar et al., 1997; Ping et al., 2014; Wang et al., 2014). Conversely, erasers, such as ALKBH9 remove the methyl group, resulting in demethylation of m6A mRNA (Duan et al., 2017; Jia et al., 2013). The m6A modification on mRNA is recognized and interpreted by readers such as YTH domain proteins, which interact with m6A sites in mRNA and facilitates the recruitment of various effector proteins and signaling molecules, thereby instigating specific effects on downstream mRNA fate (Arribas-Hernández et al., 2018; Huang et al., 2021; Scutenaire et al., 2018). As such, m6A

modification plays a crucial role in various aspects of plant growth and development, including flowering time, embryogenesis, fruit ripening, and responses to abiotic stresses such as heat, cold, viral damage, and drought in different plants (Bai et al., 2021; Han et al., 2023; Hou et al., 2022; Liu et al., 2020; Růžička et al., 2017; Song et al., 2021; Sun et al., 2022; Tzafrir et al., 2004; Wang et al., 2022a; Wang et al., 2023; Zhang et al., 2021; Zhong et al., 2008; Zhou et al., 2021).

Fruits represent a crucial component of a nutritionally balanced human diet, providing essential vitamins, antioxidants, and dietary fiber. Fruit ripening process is intricately regulated, exerting a significant influence on fruit quality. Exploring the regulatory mechanisms governing fruit ripening holds great promise for enhancing fruit quality and fostering the development of novel fruit varieties (Seymour et al., 2013; Slavin and Lloyd, 2012). Recent investigations have unveiled pervasive impacts of m6A modification on fruit ripening and senescence (Zhou et al., 2019; 2021). For instance, in typical climacteric fruits like tomato, researchers have observed a widespread occurrence of m6A methylation on fruit mRNA. Moreover, the m6A methylation at stop codons and in 3' UTRs of mRNAs demonstrates a notable negative correlation with the abundance of transcripts in fruits (Zhou et al., 2019). Additionally, during fruit ripening, the m6A RNA demethylase SlALKBH2 gradually increases, leading to elevated levels of transcripts for various ripening-associated genes, including *SlDML2* (encoding a DNA demethylase enzyme) and *Nr* (encoding an ethylene receptor protein), thereby promoting fruit ripening (Zhou et al., 2019). In non-climacteric fruits like strawberry, similar m6A modifications have also been detected. However, diverging from tomato fruit, m6A modification in strawberry is notably enriched in CDS regions, particularly after the onset of ripening. Interestingly, m6A modification within this region possesses an overall positive correlation with gene expression. Furthermore, it has been determined that m6A modification in strawberry influences fruit ripening by modulating the ABA pathway (Zhou et al., 2021). These findings enhanced our understanding of the regulatory mechanisms associated with fruit ripening. Nevertheless, further investigation is still required to ascertain how m6A impacts the ripening process and quality metabolism of different fleshy fruit species.

Kiwifruit (*Actinidia chinensis*), akin to tomato, is a climacteric fruit, and its ripening and quality formation processes are largely regulated by ethylene signaling. Over the past two decades, extensive research has revealed the intricate involvement of the ethylene pathway in the regulation of kiwifruit fruit ripening. For instance, downregulation of the expression of 1-aminocyclopropane-1-carboxylate oxidase (*ACO*), an enzyme involved in ethylene synthesis, can effectively delay fruit softening, thus modulating kiwifruit ripening (Atkinson et al., 2011). Additionally, pivotal transcription factors (TFs) such as AcEIL2 and AcEIL3 have been identified as activators that regulate the transcription of ripening-related genes, including

AcACO1 and *AcXET5* (encoding xyloglucan endotransglucosylase), providing crucial insights into the molecular basis of kiwifruit ripening (Yin et al., 2010). Recently, several studies have indicated the involvement of ethylene response factor (ERF), namely AcERF182 and AcERF91, in regulating important quality attributes of kiwifruit, such as soluble sugars and vitamin C (Chen et al., 2021; Wang et al., 2022b). These investigations have yielded valuable insights into the molecular mechanisms underlying kiwifruit fruit ripening and the development of quality attributes. However, it is important to note that the focus of these studies has primarily been on molecular breeding strategies related to genetic regulation. As a consequence, there has been a relative neglect of exploring epigenetic modifications, notably the potential influence of the highly conserved plant regulatory mechanism, m6A modification, on the regulatory processes governing fruit quality in kiwifruit.

In this study, we performed a comparative analysis of the m6A methylomes of kiwifruit at four different development and ripening stages, revealing the dynamic changes in m6A modification during kiwifruit ripening. Unlike strawberry (non-climacteric fruit), m6A modification in kiwifruit displays similar trends as seen in tomato (climacteric fruit). Specifically, we observed that a) the alterations in m6A modification of transcripts during fruit ripening are mainly concentrated in the stop codon and 3' UTRs, exhibiting a negative correlation with gene expression; b) the sequence motif for transcript m6A modification is UGUA; and c) fruit ripening is predominantly controlled by erasers rather than writers. Unlike tomato, readers also play a role in kiwifruit fruit ripening, as both the eraser AcALKBH10 (Acc10991) and the reader AcECT9 (Acc26109) influence the concentrations of accumulation of soluble sugars and organic acids, which are essential traits for fruit quality. These findings demonstrate that m6A exerts both common and distinct effects during the ripening of climacteric and non-climacteric fruits, offering a novel perspective for cultivating high-quality kiwifruit.

Materials and Methods

Plant materials

Kiwifruits (*A. chinensis* cv. Hongyang) were cultivated in the Research Orchard located in Shifang, Sichuan Province, China. To study the kiwifruit development and ripening, fruits were sampled at different stages - specifically, at 120, 160, and 185 days after pollination (DAP), as well as 5 days after harvesting at 185 DAP (185 DAP + 5). Pericarps, which refer to the fruit outer layer without skin and seeds, were collected from ten fruits of equal sizes and pooled as one biological replicate. The collected fruit tissues were cut into small pieces, quickly frozen in liquid nitrogen, and preserved in -80°C freezers. Two biological replicates were used for Methylated RNA Immunoprecipitation (MeRIP) sequencing analysis, and three biological replicates were used for transcriptome profiling in subsequent experiments.

Determination of ethylene production in kiwifruit

Ethylene quantification was conducted utilizing a GC1120 gas chromatograph (Sunny Hengping, Shanghai, China) in accordance with the previously specified comprehensive parameters (Deng et al., 2018). Three biological replicates, each comprising six fruits, were assessed at every development and ripening stages for measurements.

Determination of m6A by LC-MS/MS

Total RNA was extracted from kiwifruit fruits using a plant RNA extraction kit (BIOFIT, RN33050). mRNA was isolated from total RNA using an mRNA purification kit (Promega, Z5300). Subsequently, mRNA was digested following a previously described method (Zhou et al., 2019). Briefly, 400 ng of mRNA was digested with 2 units of ribonuclease P1 (Wako, 145-08221) in a 100 μL reaction system at 37°C for 6 hours, followed by the addition of 11 μL of 1M NH_4HCO_3 and 2 units of alkaline phosphatase (Sigma-Aldrich, P6774), and further incubation at 37°C for 6 hours. The digested samples were diluted 2-fold for LC-MS/MS analysis. Nucleosides were separated using a Thermo Hypersil Gold 100x2.1 (mm) 1.9micron column (25002-102130) and detected using an X500 QTOF mass spectrometer. The mobile phase consisted of buffer A (5 mM ammonium acetate) and buffer B (100% acetonitrile). Pure commercial standards A (TargetMol, T0853) and m6A (TargetMol, T6599) were used for calibration. The m6A/A ratio in the samples was calculated. The experiment was conducted with three independent biological replicates.

Construction of kiwifruit MeRIP sequencing library

MeRIP sequencing analysis was conducted using a previously described protocol (Dominissini et al., 2013). In brief, total RNA was isolated from kiwifruit fruit tissues using a Plant RNA Purification Reagent (Invitrogen, Carlsbad, CA, USA) and processed to prevent genomic DNA contamination and generate first-strand complementary DNA, following established procedures. Subsequently, fragmented mRNAs (5 μg) were incubated with anti-m6A polyclonal antibody (Synaptic Systems, 202003; 10 μg) in 450 μL of immunoprecipitation (IP) buffer containing 10 mM Tris-HCl, pH 7.4, 150 mM NaCl, 0.1% NP-40 (v/v), and 300 U/mL RNase inhibitor (Promega, N2112S) at 4°C for 2 hours. The mixture was then subjected to immunoprecipitation with Dynabeads Protein-A (Life Technologies, 10002A; 50 μL) at 4°C for an additional 2 hours. After washing with high-salt buffer and IP buffer, the bound mRNAs were eluted from the beads with N6-methyladenosine (Sigma, M2780; 6.7 mM) in IP buffer and recovered through phenol-chloroform extraction and ethanol precipitation. Library construction for Illumina sequencing was performed using NEBNext Ultra™ RNA library

prepare kit (NEB, E7530) with 50 ng of immunoprecipitated mRNAs or pre-immunoprecipitated mRNAs (input control).

MeRIP and transcriptome profiling analysis

The MeRIP samples underwent m6A-seq analysis as previously described (Chen et al., 2018b). Raw reads from the NovaSeq 6000 platform were quality controlled and preprocessed using Fastp (version 0.22.0) (Chen et al., 2018b) to remove adaptor sequences, low-quality reads, and short reads. The resulting clean reads were then aligned to the kiwifruit reference genome red5 using Burrows Wheeler Aligner (BWA; version 0.7.17-r1188) (Li and Durbin, 2009) with default parameters to generate alignment files. Only uniquely mapped reads with a Mapping quality (MAPQ) score of at least 30 were used for subsequent analysis.

The m6A peaks were identified using Model-based Analysis for ChIP-Seq (MACS; version 3.0.0b1) software (Zhang et al., 2008) with the corresponding input sample serving as a control. A stringent cutoff threshold for the MACS-assigned false discovery rate (FDR) of less than 0.01 was applied. Confident peaks consistently detected in both biological samples were annotated to the kiwifruit red5 annotation file using in-house python scripts. Differentially methylated peaks were determined using MetPeak (version 1.1) software (Cui et al., 2016), with a fold change of at least 1.5 and FDR of less than 0.01.

To identify m6A-enriched motifs, HOMER (Heinz et al., 2010) was used. All peaks mapped to mRNAs were considered as target sequences, and the exon sequences, except for the peak-containing sequences, were used as background sequences. The motif length was limited to six nucleotides. PyGenomeTracks (version 3.7) (Lopez-Delisle et al., 2020) was employed for visualization analysis of m6A peaks, while clusterProfiler (version 4.3) (Yu et al., 2012) was used for KEGG analysis of m6A-modified genes.

To profile the transcriptome, the alignment files of m6A-seq input samples were utilized again for generating read counts at the transcript level using featureCounts (version 2.0.3) (Liao et al., 2013). These read counts were subsequently employed to assess gene expression levels, quantified as transcripts per million (TPM). The m6A-modified transcripts underwent KEGG analysis utilizing clusterProfiler (Wu et al., 2021) The significance of enrichment was determined based on p-values ≤ 0.05. To compare genes associated with m6A modification in different kiwifruit datasets, ComplexHeatmap (Gu et al., 2016) in R software was employed.

RNA extraction and RT-qPCR analysis

Total RNA from kiwifruit tissues was extracted employing a Plant RNA Purification Reagent (Invitrogen, Carlsbad, CA, USA) according to the manufacturer's guidelines. Measures were taken to prevent genomic DNA contamination and facilitate first-strand complementary DNA

synthesis, following established protocols (Deng et al., 2018). For quantitative reverse-transcription PCR (qRT-PCR), a Bio-Rad CFX384 Real-Time System was utilized, along with 2×SYBR Green qPCR Mix (Vazyme, Q431-02), as per the manufacturer's instructions. The relative transcript level of each gene was determined using the ΔCt method, with AcActin serving as the internal control (Wang et al., 2022b). Please refer to **Supplemental Data 1** for a list of primers employed in the qRT-PCRs.

Transient overexpression and virus-induced gene silencing in kiwifruit

Related genes were transiently expressed in kiwifruit using previously described methods (Shu et al., 2023). To generate gene overexpression constructs, pBI121-AcECT9 and pBI121-AcALKBH10, the coding sequence of each gene was amplified using primers described in **Supplemental Data 1**. These amplified sequences were then inserted into the binary pBI121 vector through recombination. For the generation of virus-induced gene silencing (VIGS) constructs, specifically pTRV2-AcECT9 and pTRV2-AcALKBH10, the partial coding sequence of each gene was amplified using specific primers provided in **Supplemental Data 1**. The amplified sequences were subsequently cloned into the pTRV2/pTRV1 vector system based on the Tobacco rattle virus. Following transformation, all constructs were individually introduced into Agrobacterium tumefaciens GV3101. The gene sequences within each construct were verified using Sanger sequencing.

To transiently overexpress or silence genes in kiwifruits, a total of 30 fruits attached to vines at 120 days after pollination (DAP) were selected. These fruits were injected at a depth of approximately 0.5 cm into the pericarp tissues using 0.1 ml of agrobacterium culture (at 1.0 OD600) harboring the respective overexpression or VIGS constructs. Negative controls were performed using empty pBI121 or pTRV2/pTRV1 vectors. After 7 days of agroinfiltration (i.e., at 127 DAP), the infiltrated fruits were harvested, and the outer pericarps were collected. The collected pericarps were rapidly frozen in liquid nitrogen and stored at -80 °C for subsequent molecular analyses.

Determination of soluble sugars and organic acids in kiwifruit/tomato

Fresh tomato fruit or kiwifruit powder was weighed to 0.1 grams and 1 milliliter of 50% acetonitrile (ACN: H2O) was added. The mixture was vigorously vortexed to ensure thorough mixing, followed by ultrasonication for 1 hour at low temperature. Subsequently, the mixture was centrifuged at 13,000 rpm for 10 minutes, and the supernatant were collected for dilution (kiwifruit samples were diluted to 600-fold, tomato samples are diluted to 200-fold). After filtration through a 0.22 μm filter, the samples were transferred to brown sample vials for UPLC analysis. Organic acids were extracted using 50% methanol by a similar procedure, with tomato

fruit extracts diluted to 400-fold and kiwifruit extracts diluted to 600-fold for measurement. Quantitative analysis of soluble sugars and organic acids was performed using the SCIEX Triple Quad 5500 LC-MS/MS system, employing an ACQUITY UPLC BEH Amide column (1.7 μm, 2.1 x 100 mm, manufactured in Ireland) for compound separation and quantification. Data processing involved using the concentration values (expressed in μg/ml) obtained from the instrument test report. The calculation formula for determining the final concentration (mg/g FW, fresh weight) was as follows: final concentration (mg/g FW) = instrument test concentration * dilution factor * 10 * 0.001.

m6A-IP-qPCR experiments

The m6A-IP-qPCR was performed as described (Zhou et al., 2019). Briefly, mRNA was isolated and purified from total RNA according to manufacturer's instrunctions (Promega, Z5200). 5 μg of mRNA were incubated in fragmentation buffer at 94 °C for 2 minutes for converting into nucleic acid fragments with a length of about 300 nt. mRNA fragments were purified using the standard ethanol precipitation method, dissolved in 250 μl DEPC water, with 5 μl reserved as Input. mRNA fragments were then combined with anti-m6A polyclonal antibody (Synaptic Systems, 202003) in IP buffer and rotated at 4°C for 2 hours. Next, the mixture was immunoprecipitated with Dynabeads Protein-A magnetic beads (Thermo, 10001D) at 4°C for 2 hours. The magnetic beads were washed separately with high-salt buffer and IP buffer. Subsequently, m6A nucleoside was introduced at a concentration of 6.7 mM, and the solution was rotated at 4°C for 2 hours to displace m6A-modified mRNA fragments. mRNA fragments were purified again using the standard ethanol precipitation method, dissolved in an appropriate amount of DEPC water, and stored on ice. M-MLV reverse transcriptase (Takara, 2640A) and random primers were employed for cDNA reverse transcription of post-immunization mRNA and pre-immunization mRNA (Input mRNA), followed by RT-qPCR analysis using primers designed near the m6A peak. Cycle threshold (CT) $2^{(-\Delta CT)}$ method was used to calculate the enrichment of m6A (Schmittgen & Livak, 2008). The value for the immunoprecipitated sample was normalized against that for *AcACTIN*. All primers used for m6A-IP-qPCR are listed in **Supplementary Data 1**.

Heterologous expression of AcALKBH10 in tomato and growth conditions

The full-length coding sequence of *AcALKBH10* amplified from the kiwifruit cDNA library was ligated into the 35S:pBI121 vector to generate 35S:pBI121-*AcALKBH10*. The construct was transformed into Agrobacterium (strain GV3101), and the T0 transgene was obtained in Micro-Tom tomato using *Agrobacterium tumefaciens*-mediated genetic transformation. Transformed lines were screened by PCR with *AcALKBH10*-specific primers and on media containing kanamycin. The growth conditions of AcALKBH10 heterologous transgenic lines

and wild-type tomato plants were the same as previously described except light intensity (200-μmol m^{-2} s^{-1}) (Deng et al., 2022). Tomato fruit samples harvested at different development and ripening stages of 36DPA, 42DPA, Br and Br+7 were stored at -80 °C until use.

Phylogenetic analysis

The clustalw algorithm was employed within the MEGA X software (Kumar et al., 2018) to facilitate protein sequence alignment, resulting in precise alignment outcomes that were subsequently utilized for the construction of a comprehensive molecular phylogenetic tree. To ensure robustness and accuracy, the maximum likelihood model was meticulously applied during this process, accompanied by a bootstrap value of 1000.

Statistics

In order to evaluate the comparison between individual treatments and their respective controls, paired two-tailed Student's *t*-tests were performed using the R software. A significance level of $p \leq 0.05$ was adopted to indicate statistical significance in this analysis. Furthermore, ggplot2, a widely employed data visualization package in the R software was utilized to visually represent the outcomes of these statistical analyses (Wickham, 2016).

Results

The m6A levels display a gradual decrease during kiwifruit ripening process

To reveal whether mRNA N6-methyladenine (m6A) is involved in the regulation of fruit ripening in kiwifruit, pericarp tissues at 4 fruit development and ripening stages including 120, 160, 185 days after pollination (DAP) and 5 days after harvest at 185 DAP (185 DAP + 5) were collected to perform Methylated RNA Immunoprecipitation (MeRIP) sequencing (**Fig. 1a**). Ethylene content changed in harvest kiwifruit fruits from 185 to 185 DAP + 13, started at 185 DAP + 1 and reached its peak at 185 DAP + 5 (**Fig. 1b**). After adapter trimming and reads filtration, we generated 14-26 million clean reads for each m6A sequencing sample from raw reads, which were generated by the m6A library of kiwifruit samples according to the standard m6A-seq protocol. The sequencing depth for our m6A samples was comparative to that observed in others fruits, such as tomato (19-28 million reads, 900 Mb) (Sato et al., 2012; Zhou et al., 2019) and strawberry (24-37 million reads, 240 Mb) (Edger et al., 2019; Zhou et al., 2021), and 91-96% reads were uniquely aligned to the kiwifruit reference genome Red 5 (653 Mb) (Wu et al., 2019) (**Supplemental Data 2**). Moreover, high Pearson Correlation Coefficients (PCC) were also observed in our m6A and its parallel RNA-Seq biological replicates, respectively (**Fig. S1**). The expression level of kiwifruit ripening marker genes *AcACS (Acc05955)*, *AcACO1 (Acc24995)* and *AcACO2 (Acc20538)* were consistent both in

RNA-Seq and qPCR experiments that were corresponded to the appearance of ethylene peaks (**Fig. 1b; Fig. S2**).

Next, m6A methylated peaks in kiwifruit fruit were identified by the macs3 callpeak subroutine with a false discovery rate (FDR) < 0.01, and only those methylated peaks that were consistently detected in all two biological replicates are considered reliable and used for subsequent analysis. Finally, 27433, 24755, 21445, and 16414 m6A peaks associated with 16295, 15948, 15052, and 12785 transcripts in fruit pericarps with 120, 160, 185, and 185 DAP + 5 were identified, respectively (**Fig. 1c, d; Supplemental Data 3**). Interestingly, the number of transcripts containing one or more m6A peaks decreases gradually as the kiwifruit ripening (**Fig. 1d**), showing that the level of m6A in kiwifruit gradually decrease when the fruit ripening. Furthermore, evaluating the mRNA m6A methylation levels in kiwifruit by LC-MS/MS across the four stages also revealed a decline in overall mRNA m6A levels during fruit ripening process (**Fig. 1e**), further supporting the negative correlation between m6A levels and fruit ripening. Besides, combined with the genes expression (**Supplemental Data 4**) and m6A peaks results, we estimated that each actively expressed transcript (transcripts per kilobase of exon model per million mapped reads, TPM > 1) contains 0.6 - 0.9 m6A methylated peaks in the transcriptome of kiwifruit pericarp (**Supplemental Data 5**). Further KEGG enrichment analysis showed that these actively expressed transcripts with m6A modification were involved in RNA degradation pathway, mRNA surveillance pathway, RNA transport pathways, ribosome pathways etc. (**Supplemental Fig. S3; Supplemental Data 6**), which also demonstrating that m6A modification is a common feature of mRNA in kiwifruit ripening.

m6A modifications occur predominantly at the stop codons and the 3'-UTRs

To deepen our understanding of the function of m6A in kiwifruit ripening, an analysis of its distribution at the transcriptome-wide level was conducted. Corresponding to the structure of mature mRNA, the kiwifruit transcripts was arbitrarily separated into five non-overlapping segments, i.e., 5'-UTR, start codon (100-nucleotides window centered on the start codon), coding sequence (CDS), stop codon (100-nucleotides window centered on the stop codon), and 3'-UTR. It was shown that m6A modifications in all four development and ripening stages in kiwifruit are predominantly enriched around stop codons and within the 3' UTR, however, the proportion of m6A peaks in these regions shows an increasing trend along with the fruit ripening progression, especially at from 185 to 185 DAP + 5 (**Fig. 2a**).

Furthermore, the ratio diagram of m6A enrichment revealed that the percentage of m6A peak falling into the 3' UTRs increased from 51.4 % to 63.8 % from 185 to 185 DAP + 5, and displayed a slight increase from 120 to 185 DAP (**Fig. 2b**). In comparison, the percentage of m6A peaks locating in the CDS region decreased from 22.9 % to 13.0 %, respectively, from

185 to 185 DAP + 5, with a slight decrease observed from 120 to 185 DAP **(Fig. 2b)**. Additionally, the relative ratio of m6A within the 3' UTRs increased significantly, while the relative ratio of m6A within the CDS region decreased significantly from 185 to 185 DAP + 5. (**Fig. 2c**). Following this, we identified the high-confidence sequence motif UGUA during kiwifruit ripening by using Hypergeometric Optimization of Motif EnRichment (HOMER), where symbols U and G represents uridine and guanosine, respectively, while the underlined A signifies m6A (**Fig. 2d; Fig. S4**).

m6A modifications and gene expression levels exhibit an inverse correlation during ripening

In order to explore the association between mRNA and m6A methylation level during kiwifruit ripening, we employed MetPeak software with fold change ≥ 1.5 and FDR (False Discovery Rate) < 0.01 to recognize uniquely methylated peaks over three intervals - from 120 to 160 DAP, 160 to 185 DAP, and 185 to 185 DAP + 5 - and successfully uncovered 1310 hypermethylated (up-regulated in 160 DAP) and 507 hypomethylated (down-regulated in 160 DAP), 1049 hypermethylated (up-regulated in 185 DAP) and 973 hypomethylated (down-regulated in 185 DAP), and 923 hypermethylated (up-regulated in 185 DAP + 5) and 1560 hypomethylated (down-regulated in 185 DAP + 5) peaks (**Fig. S5; Supplemental Data 7**), respectively. Subsequently, a comparative analysis was conducted on the set of differentially methylated transcripts between 160 and 185 DAP. The primary objective of this analysis was to identify differentially expressed genes (fold change ≥ 1.5; P value < 0.01). The observations divulged that within the 913 hypermethylated transcripts (up-regulated in 160 DAP), only 102 demonstrated increased expression levels, while 376 exhibited decreased expression levels (**Fig. 3a**). Similarly, among the 1004 hypomethylated transcripts (up-regulated in 185 DAP), 278 exhibited augmented expression levels, and 98 presented diminished expression levels (**Fig. 3a**). Furthermore, analogous outcomes were observed in the case of hypomethylated transcripts during the periods of 120 to 160 DAP (**Fig. S6a**), as well as for both hypermethylated and hypomethylated transcripts between 185 and 185 DAP + 5 (**Fig. 3b**). These results present herein suggest that there exists a negative correlation between the prevalence of m6A and the relative abundance of the transcripts.

To elaborate on the analysis of the association between mRNA expression and m6A modification, we extended this analysis to the entire transcriptome with all m6A modified genes. Indeed, the cumulative distribution of gene expression ratio changes and the gene expression ratio depicted in the box plot across fruit stages of 120 to 160 DAP (**Fig. S6b**), 160 to 185 DAP (**Fig. 3c**), and 185 to 185 DAP + 5 (**Fig. 3d**) indicated that transcripts with more or less m6A modification demonstrated a propensity for lower or higher expression. Furthermore, plotting

the genes containing differential m6A peaks in various segments against their expression levels served to verify the inverse correlation between m6A modifications and gene expression levels (**Fig. 3e, f; Fig. S6c**).

m6A modification negatively modulates the expression of ripening-related genes

During the process of kiwifruit ripening, the activation and expression of ripening-related genes is a crucial step. To investigate the potential involvement of m6A modification in the regulation of ripening-related genes, we screened genes exhibiting differential expression and differential m6A modification levels at various fruit ripening stages. Through this analysis, we identified six fruit ripening-related genes, namely *Acc27491* (encoding an ethylene receptor-like protein), *Acc04179* (encoding an ethylene receptor-like protein), *Acc23267* (encoding a sugar transport protein), *Acc25497* (encoding a sucrose synthase), *Acc12764* (encoding a beta-galactosidase that promotes fruit softening), and *Acc09209* (encoding an abscisic acid receptor-like protein homologous to PYL9 that promotes fruit ripening in tomato). As we expected, alterations of kiwifruit ethylene receptors in transcript abundance and m6A modification observed exhibited a pattern akin to its tomato homologous gene *NR* in fruit ripening (Fig. 4a; Zhou et al., 2019). The m6A peaks of *Acc27491* and *Acc04179* were enriched near the 3' UTRs and showed a declining trend from 160 to 185 DAP + 5, while its transcript abundance gradually increased at this stage (**Fig. 4a, b**). Further quantitative polymerase chain reaction (qPCR) and m6A immunoprecipitation coupled with qPCR (m6A-IP-qPCR) experiments confirmed this negative regulatory relationship between m6A modification of kiwifruit ethylene receptors and its gene expression (**Fig. 4a, b**). Moreover, the m6A peaks of sucrose accumulation-related genes *Acc23267* and *Acc25497* were enriched in the 3' UTRs and 5' UTRs, respectively. Further transcript quantification and m6A-IP-qPCR experiments also confirmed that the m6A modification of these transcripts and their expression was negatively correlated from 185 to 185 DAP + 5 (**Fig. 4c, d**). Similar to the four genes described above, the abundance of *Acc12764* and *Acc09209* transcripts also showed a negative regulatory relationship with their methylation modification levels (**Fig. S7a, b**).

AcALKBH10 affects fruit ripening and flavor quality in kiwifruit

Following the identification of alterations in m6A levels in a significant number of ripening-related genes in kiwifruit (**Fig. 4; Fig. S7**), we proceeded to investigate the underlying mechanisms responsible for these changes. To this end, we utilized the protein sequences of m6A RNA writers (mRNA adenosine methylase, MTA/ MTB/ MTC; FKBP12 interacting protein 37, FIP37; HAKAI; virilizer, VIR), readers (YTH domain family protein, ECT), and erasers (AlkB homolog, ALKBH) from Arabidopsis and tomato as a reference, and identified corresponding homologous proteins of writers, readers, and erasers in kiwifruit (**Fig. S8**).

Further analysis of gene expression heatmaps revealed that the RNA demethylase *AcALKBH10* was notably upregulated during fruit ripening, while the RNA methylation reader *AcECT9* was specifically downregulated during the same period (**Fig. 5a**).

Subsequently, transient overexpression and silencing of *AcALKBH10* were conducted in kiwifruit at 120 DAP (**Fig. 5b**). Metabolites determination demonstrated a significant increase in the levels of glucose, fructose, and sucrose, and a significant decrease in citric acid levels in *AcALKH10*-overexpressing lines compared to control lines. In contrast, the *AcALKBH10*-silencing lines exhibited a reversed pattern (**Fig. 5c**). Additionally, RT-qPCR analysis revealed that the overexpression of *AcALKH10* resulted in upregulation of several fruit-ripening genes, including Acc27491, Acc25497, Acc23267, Acc12764, Acc04179, and Acc09209, whereas their expression was decreased in the *AcALKBH10*-silencing lines (**Fig. 5d**). Moreover, the prospective role of *AcECT9* in kiwifruit was also explored using a similar methodology (**Fig. 5e**). However, the metabolic assays exhibited a significant reduction in glucose, fructose, and sucrose levels in the *AcECT9*-overexpression lines as opposed to the control line, whereas no contrary effect was observed in the *AcECT9*-silencing lines (**Fig. 5f**). Correspondingly, RT-qPCR assays demonstrated a down-regulation trend in fruit ripening-related genes in *AcECT9*-silencing lines and an up-regulation trend in *AcECT9*-overexpression lines, although the effects were mostly non-significant (**Fig. 5g**). In light of these findings, it can be inferred that mRNA demethylase AcALKBH10 may chiefly govern m6A levels of kiwifruit ripening-related genes, which, in turn, modulates fruit flavor quality by regulating the concentration of soluble sugars and acids in the fruit.

Heterologous expression of *AcALKBH10* in tomato accelerates fruit ripening and flavor quality

To gain a deeper understanding of AcALKBH10 function, we expressed this gene in climacteric fruit research model tomato (**Fig. S9a**). As shown in **Fig. 6a and Fig. S9b,** overexpression of *AcALKBH10* accelerated fruit ripening in tomato. This inference was further supported by the soluble solid content in tomato fruits at the Br+15 stage, as well as the time from flower anthesis to the fruit breaker (BR), as depicted in **Fig. S9c** and **Fig. S9d**. Additionally, our analysis of fruit metabolites at BR + 7 showed that AcALKBH10 modulated fruit quality by regulating the content of soluble sugars and acids (**Fig. 6b**).

To elucidate how AcALKBH10 affects tomato fruit ripening and quality, we analyzed the expression levels of various genes involved in tomato fruit ripening, including *SlETR3* and *SlETR4* (homologous to *Acc27491* and *Acc04179*), *SlSTP18* (homologous to *Acc23267*), *SlPYL9* (homologous to *Acc09209*), *SlTBG4* (homologous to *Acc12764*), and other fruit-ripening genes such as *ACS2*, *ACS4*, *ACO1*, *SlALKBH2*, *DML2*, and *RIN* in both wild type and

AcALKBH10-overexpressed lines at 36, 42 DPA(days post anthesis), and BR + 3 (**Fig. 6c-e)**. We found that expression levels of these fruit-ripening genes were significantly higher in the *AcALKBH10*-overexpressed lines compared to the wild type both before and after fruit breaker stages. Taken together, our findings suggest that AcALKBH10 can regulate fruit ripening and fruit quality by modulating the expression of ripening-related genes.

Discussion

Epigenetic modifications, notably the m6A modification, exhibit diverse functions in plant growth and development, including organogenesis, flowering, embryogenesis, root development, and fruit ripening (Chen et al., 2018a; Duan et al., 2017; Růžička et al., 2017; Zhou et al., 2019). Despite the considerable research conducted on m6A modification and its molecular regulatory mechanisms in diverse physiological processes of plants, a comprehensive understanding of the specific effects of m6A modification on fruit ripening and quality formation remains limited, especially in the context of kiwifruit, which exhibits a typical postharvest ripening and is valued for its substantial nutritional content to consumers. Here, through comparative analysis of the m6A methylomes in kiwifruit fruits at four different stages, we observed dynamic changes in m6A modification during the fruit ripening process. As fruits were ripened, the levels of m6A modification gradually decreased (**Fig. 1c, d**), while the abundance of transcripts related to fruit ripening concurrently increased (**Fig. S2**). Moreover, like the observations in tomato and strawberry fruits (Zhou et al., 2021; Zhou et al., 2019), m6A modifications in kiwifruit were predominantly enriched in proximity to stop codons and within the 3' UTRs (**Fig. 2**), exhibiting a negative correlation with gene expression (**Fig. 3**). These findings suggest that the m6A modification within mRNA represents a prevalent modification, displaying a degree of functional conservation during the process of fruit ripening.

Interestingly, a positive influence of m6A deposition in the CDS region on mRNA abundance was found during the ripening process of strawberry fruit (Zhou et al., 2021), which was not observed in tomato (Zhou et al., 2019) and kiwifruit, suggesting that the connection between mRNA m6A modification and its expression may exhibit distinctive characteristics in the ripening processes of different fleshy fruits. In kiwifruit, as fruit ripening progresses, there is an increasing trend in the proportion of m6A peaks (**Fig. 2b**), which differs from the results observed in tomato and strawberry (Zhou et al., 2021; Zhou et al., 2019). At the onset of ripening, the proportion of m6A peaks in tomato does not significantly change, while in strawberry, there is a substantial increase in m6A peak proportion within the CDS region. These results support that the m6A modification within mRNA exhibits a degree of functional divergence during ripening process of different fruits.

In tomato fruit, the m6A demethylase SlALKBH2 was shown to be involved in fruit ripening through binding the mRNA of the DNA demethylase gene *SlDML2*, a key ripening regulator in tomato (Zhou et al., 2019). Similarly, we found that the RNA demethylase AcALKBH10 predominantly governs the expression levels of kiwifruit ripening-related genes. However, such regulatory mechanisms were not observed in strawberry fruit (Zhou et al., 2021). Instead, methyltransferases MTA and MTB were found to impact strawberry fruit ripening by modulating the abscisic acid (ABA) pathway (Zhou et al., 2021). These findings highlight substantial variations in the regulatory mechanisms of m6A modification during fruit ripening between climacteric and non-climacteric fruits. Additionally, even among climacteric fruits such as tomato and kiwifruit, the modes of m6A modification-mediated regulation of fruit ripening manifest subtle differences. Specifically, in kiwifruit, there is a progressive increase in the abundance of m6A peaks in specific genomic regions during fruit ripening (**Fig. 2a**), in contrast to the stable ratio observed in tomato fruit (Zhou et al., 2019). It is worth noting that kiwifruit exhibits much higher ethylene production compared to tomato during ripening process, it is possible that the differences in m6A modification in climacteric fruits might be correlated to the rate of ethylene production. Nonetheless, comprehensive investigations are warranted to validate and gain a deeper understanding of the underlying mechanisms pertaining to this aspect.

An increasing body of evidence indicates that epigenetic modifications including both DNA methylation and 6mA modification play a pivotal role in the intricate process of fruit ripening (Ecker, 2013; Giovannoni et al., 2017; Ji and Wang, 2023). Moreover, it was shown that there is a crosstalk between 5mC and 6mA methylations during fruit ripening process in tomato (Zhou et al., 2019). Although the involvement of m6A modification in regulation of the ripening and flavor quality in kiwifruit was uncovered in this study, the putative role and mode of action of DNA methylation during kiwifruit ripening remain unknown. Moreover, whether the interaction between m6A and DNA methylation is conserved in kiwifruit like in tomato necessitate additional exploration.

In conclusion, our study conducted a systematic investigation of the temporal dynamics of m6A modification during kiwifruit ripening, yielding a comprehensive elucidation of the regulatory mechanisms governing kiwifruit quality in fruit ripening through m6A modification. Additionally, the functional characterization of key epigenetic modifiers, such as the eraser AcALKBH10 and the reader AcECT9, in influencing the accumulation of essential metabolites like soluble sugars and organic acids further emphasizes the potential of epigenetic modifications as targets for breeding high-quality kiwifruit varieties. By elucidating the regulatory mechanisms of m6A modification in fruit ripening, our study provides a solid foundation for future breeding efforts aimed at enhancing fruit quality, nutritional content, and market appeal. In summary, our study not only unveils the nuanced landscape of epigenetic

modifications during kiwifruit ripening but also underscores their pivotal role in shaping fruit quality traits. This knowledge bridges the gap between fundamental epigenetic insights and practical breeding applications, paving the way for the development of superior kiwifruit varieties with enhanced flavor, nutritional content, and market appeal.

Acknowledgments

This research was funded by the Natural Science Foundation of Sichuan Province, China (2023NSFSC1991), the Outstanding Young Scientific and Technological Talents of Sichuan Province (2022JDJQ0057), the Applied Basic Research Category of Science and Technology Program of Sichuan Province (2021YFYZ0010; 2021YFQ0071), the Institutional Research Fund of Sichuan University (2022SCUNL105), the Open Project Program of Key Laboratory of Breeding and Utilization of Kiwifruit in Sichuan Province(MSZKF202301), the Sichuan Provincial Academy of Natural of Natural Resource Sciences, and the Fundamental Research Funds for the Central Universities (SCU2024D003), the fund for strategic cooperation between Sichuan University and Dazhou Municipal Government (2021CDDZ-16), the fund for Postdoctoral Science Foundation of Sichuan Province (TB2022076).

Competing interests

All authors declare no competing interests.

Author contributions

M.Liu, P.S., D.S. and K.L. designed the experiments; D.S., P.S., Y.C., Y.W., H.D., X.D., X.Z. and R.W. conducted the experiments; P.S., D.S., N.H., H.L., Y.Z., D.L., Y.X. and M.Li analyze the data; M.Liu., P.S. and D.S. wrote the paper with the input of all the authors. Y.H. revised and improved the manuscript. All authors have approved this manuscript.

Data availability

The MeRIP sequencing datasets have been deposited in the Genome Sequence Archive at the National Genomics Data Center, Beijing Institute of Genomics, Chinese Academy of Sciences (http://bigd.big.ac.cn). The assigned accession number for the datasets is CRA011218, and they are accessible to the public.

References

Arribas-Hernández L, Bressendorff S, Hansen MH, Poulsen C, Erdmann S, Brodersen PJTPC. 2018. An m6A-YTH module controls developmental timing and morphogenesis in Arabidopsis. *Plant Cell* **30**(5): 952-967.

Arribas-Hernández L, Brodersen P. 2020. Occurrence and Functions of m(6)A and Other Covalent Modifications in Plant mRNA. *Plant Physiology* **182**(1): 79-96.

Atkinson RG, Gunaseelan K, Wang MY, Luo L, Wang T, Norling CL, Johnston SL, Maddumage R, Schröder R, Schaffer RJ. 2011. Dissecting the role of climacteric ethylene in kiwifruit (Actinidia chinensis) ripening using a 1-aminocyclopropane-1-carboxylic acid oxidase knockdown line. *Journal of Experimental Botany* **62**(11): 3821-3835.

Bai C, Fang M, Zhai B, Ma L, Fu A, Gao L, Kou X, Meng D, Wang Q, Zheng S, et al. 2021. Regulations of m6A methylation on tomato fruit chilling injury. *Horticultural Plant Journal* **7**(5): 434-442.

Bokar JA, Shambaugh ME, Polayes D, Matera AG, Rottman FMJR. 1997. Purification and cDNA cloning of the AdoMet-binding subunit of the human mRNA (N6-adenosine)-methyltransferase. *Rna* **3**(11): 1233-1247.

Chen M, Urs MJ, Sánchez-González I, Olayioye MA, Herde M, Witte C-PJTPC. 2018a. m6A RNA degradation products are catabolized by an evolutionarily conserved N6-methyl-AMP deaminase in plant and mammalian cells. *Plant cell* **30**(7): 1511-1522.

Chen S, Zhou Y, Chen Y, Gu J. 2018b. fastp: an ultra-fast all-in-one FASTQ preprocessor. *Bioinformatics* **34**(17): i884-i890.

Chen Y, Shu P, Wang R, Du X, Xie Y, Du K, Deng H, Li M, Zhang Y, Grierson D, et al. 2021. Ethylene response factor AcERF91 affects ascorbate metabolism via regulation of GDP-galactose phosphorylase encoding gene (AcGGP3) in kiwifruit. *Plant science: an international journal of Experimental Plant Biology* **313**: 111063.

Cui X, Meng J, Zhang S, Chen Y, Huang Y. 2016. A novel algorithm for calling mRNA m6A peaks by modeling biological variances in MeRIP-seq data. *Bioinformatics* **32**(12): i378-i385.

Deng H, Chen Y, Liu Z, Liu Z, Shu P, Wang R, Hao Y, Su D, Pirrello J, Liu Y, et al. 2022. SlERF.F12 modulates the transition to ripening in tomato fruit by recruiting the co-repressor TOPLESS and histone deacetylases to repress key ripening genes. *Plant Cell* **34**(4): 1250-1272.

Deng H, Pirrello J, Chen Y, Li N, Zhu S, Chirinos X, Bouzayen M, Liu Y, Liu M. 2018. A novel tomato F-box protein, SlEBF3, is involved in tuning ethylene signaling during plant development and climacteric fruit ripening. *The Plant Journal* **95**(4), 648-658.

Dominissini D, Moshitch-Moshkovitz S, Salmon-Divon M, Amariglio N, Rechavi G. 2013. Transcriptome-wide mapping of N(6)-methyladenosine by m(6)A-seq based on immunocapturing and massively parallel sequencing. *Nat Protoc* **8**(1): 176-189.

Duan H-C, Wei L-H, Zhang C, Wang Y, Chen L, Lu Z, Chen PR, He C, Jia GJTPC. 2017. ALKBH10B is an RNA N 6-methyladenosine demethylase affecting Arabidopsis floral transition. *Plant Cell* **29**(12): 2995-3011.

Ecker JR. 2013. Epigenetic trigger for tomato ripening. *Nature Biotechnology* **31**(2): 119-120.

Edger PP, Poorten TJ, VanBuren R, Hardigan MA, Colle M, McKain MR, Smith RD, Teresi SJ, Nelson ADL, Wai CM, et al. 2019. Origin and evolution of the octoploid strawberry genome. *Nature Genetics* **51**(3): 541-547.

Giovannoni J, Nguyen C, Ampofo B, Zhong S, Fei Z. 2017. The Epigenome and Transcriptional Dynamics of Fruit Ripening. *Annual review of plant biology* **68**: 61-84.

Gu Z, Eils R, Schlesner M. 2016. Complex heatmaps reveal patterns and correlations in multidimensional genomic data. *Bioinformatics* **32**(18): 2847-2849.

Han R, Shoaib Y, Cai J, Kang H. 2023. ALKBH10B-mediated m6A demethylation is crucial for drought tolerance by affecting mRNA stability in Arabidopsis. *Environmental and Experimental Botany* **209**: 105306.

Heinz S, Benner C, Spann N, Bertolino E, Lin YC, Laslo P, Cheng JX, Murre C, Singh H, Glass CK. 2010. Simple combinations of lineage-determining transcription factors prime cis-regulatory elements required for macrophage and B cell identities. *Molecular Cell* **38**(4): 576-589.

Hou N, Li C, He J, Liu Y, Yu S, Malnoy M, Mobeen Tahir M, Xu L, Ma F, Guan Q. 2022. MdMTA-mediated m(6) A modification enhances drought tolerance by promoting mRNA stability and translation efficiency of genes involved in lignin deposition and oxidative stress. *New Phytologist* **234**(4): 1294-1314.

Huang W, Chen T-Q, Fang K, Zeng Z-C, Ye H, Chen Y-Q. 2021. N6-methyladenosine methyltransferases: functions, regulation, and clinical potential. *Journal of Hematology & Oncology* **14**(1): 117.

Ji Y, Wang A. 2023. Recent advances in epigenetic triggering of climacteric fruit ripening. *Plant physiology* **192**(3): 1711-1717.

Jia G, Fu Y, He CJTiG. 2013. Reversible RNA adenosine methylation in biological regulation. *Trends in Genetics* **29**(2): 108-115.

Klee HJ, Giovannoni JJ. 2011. Genetics and control of tomato fruit ripening and quality attributes. *Annual Review of Genetics* **45**: 41-59.

Kumar S, Stecher G, Li M, Knyaz C, Tamura K. 2018. MEGA X: Molecular Evolutionary Genetics Analysis across Computing Platforms. *Molecular Biology and Evolution* **35**(6): 1547-1549.

Lang Z, Wang Y, Tang K, Tang D, Datsenka T, Cheng J, Zhang Y, Handa AK, Zhu JK. 2017. Critical roles of DNA demethylation in the activation of ripening-induced genes and inhibition of ripening-repressed genes in tomato fruit. *PNAS* **114**(22): E4511-e4519.

Li H, Durbin R. 2009. Fast and accurate short read alignment with Burrows-Wheeler transform. *Bioinformatics* **25**(14): 1754-1760.

Liao Y, Smyth GK, Shi W. 2013. featureCounts: an efficient general purpose program for assigning sequence reads to genomic features. *Bioinformatics* **30**(7): 923-930.

Liu G, Wang J, Hou X. 2020. Transcriptome-Wide N(6)-Methyladenosine (m(6)A) Methylome Profiling of Heat Stress in Pak-choi (Brassica rapa ssp. chinensis). *Plants (Basel)* **9**(9).

Lopez-Delisle L, Rabbani L, Wolff J, Bhardwaj V, Backofen R, Grüning B, Ramírez F, Manke T. 2020. pyGenomeTracks: reproducible plots for multivariate genomic datasets *Bioinformatics* **37**(3): 422-423.

Luo JH, Wang Y, Wang M, Zhang LY, Peng HR, Zhou YY, Jia GF, He Y. 2020. Natural Variation in RNA m(6)A Methylation and Its Relationship with Translational Status. *Plant Physiology* **182**(1): 332-344.

Ping X-L, Sun B-F, Wang L, Xiao W, Yang X, Wang W-J, Adhikari S, Shi Y, Lv Y, Chen Y-SJCr. 2014. Mammalian WTAP is a regulatory subunit of the RNA N6-methyladenosine methyltransferase. *Cell research* **24**(2): 177-189.

Růžička K, Zhang M, Campilho A, Bodi Z, Kashif M, Saleh M, Eeckhout D, El-Showk S, Li H, Zhong S, et al. 2017. Identification of factors required for m(6)A mRNA methylation in Arabidopsis reveals a role for the conserved E3 ubiquitin ligase HAKAI. *New Phytologist* **215**(1): 157-172.

Sato S, Guigó Serra R, Cámara F, Gianese S, Consortium TG. 2012. The tomato genome sequence provides insights into fleshy fruit evolution. *Nature* **485**, 635-641

Scutenaire J, Deragon J-M, Jean V, Benhamed M, Raynaud C, Favory J-J, Merret R, Bousquet-Antonelli CJTPC. 2018. The YTH domain protein ECT2 is an m6A reader required for normal trichome branching in Arabidopsis. *Plant Cell* **30**(5): 986-1005.

Schmittgen TD, Livak KJ. 2008. Analyzing real-time PCR data by the comparative CT method. *Nature Protocols* **3**(6): 1101-1108

Seymour GB, Østergaard L, Chapman NH, Knapp S, Martin C. 2013. Fruit development and ripening. *Annual Review of Plant Biology* **64**: 219-241.

Shu P, Zhang Z, Wu Y, Chen Y, Li K, Deng H, Zhang J, Zhang X, Wang J, Liu Z, et al. 2023. A comprehensive metabolic map reveals major quality regulations in red-flesh kiwifruit (Actinidia chinensis). *New Phytologist* **238**(5): 2064-2079.

Slavin JL, Lloyd B. 2012. Health benefits of fruits and vegetables. *Advances in Nutrition (Bethesda, Md.)* **3**(4): 506-516.

Song P, Yang J, Wang C, Lu Q, Shi L, Tayier S, Jia G. 2021. Arabidopsis N(6)-methyladenosine reader CPSF30-L recognizes FUE signals to control polyadenylation site choice in liquid-like nuclear bodies. *Molecular Plant* **14**(4): 571-587.

Sun B, Bhati KK, Song P, Edwards A, Petri L, Kruusvee V, Blaakmeer A, Dolde U, Rodrigues V, Straub D, et al. 2022. FIONA1-mediated methylation of the 3' UTR of FLC affects FLC transcript levels and flowering in Arabidopsis. *PLoS Genetics* **18**(9): e1010386.

Tang D, Gallusci P, Lang ZJNP. 2020. Fruit development and epigenetic modifications. *New Phytologist* **228**(3): 839-844.

Teyssier E, Bernacchia G, Maury S, How Kit A, Stammitti-Bert L, Rolin D, Gallusci P. 2008. Tissue dependent variations of DNA methylation and endoreduplication levels during tomato fruit development and ripening. *Planta* **228**(3): 391-399.

Tzafrir I, Pena-Muralla R, Dickerman A, Berg M, Rogers R, Hutchens S, Sweeney TC, McElver J, Aux G, Patton D, et al. 2004. Identification of genes required for embryo development in Arabidopsis. *Plant Physiology* **135**(3): 1206-1220.

Wang L, Zhuang H, Fan W, Zhang X, Dong H, Yang H, Cho J. 2022a. m6A RNA methylation impairs gene expression variability and reproductive thermotolerance in Arabidopsis. *Genome Biology* **23**(1): 244.

Wang R, Shu P, Zhang C, Zhang J, Chen Y, Zhang Y, Du K, Xie Y, Li M, Ma T, et al. 2022b. Integrative analyses of metabolome and genome-wide transcriptome reveal the regulatory network governing flavor formation in kiwifruit (Actinidia chinensis). *New phytologist* **233**(1): 373-389.

Wang S, Wang H, Xu Z, Jiang S, Shi Y, Xie H, Wang S, Hua J, Wu Y. 2023. m6A mRNA modification promotes chilling tolerance and modulates gene translation efficiency in Arabidopsis. *Plant Physiology* **192**(2): 1466-1482.

Wang Y, Li Y, Toth JI, Petroski MD, Zhang Z, Zhao JCJNcb. 2014. N 6-methyladenosine modification destabilizes developmental regulators in embryonic stem cells. *Nature cell biology* **16**(2): 191-198.

Wei LH, Song P, Wang Y, Lu Z, Tang Q, Yu Q, Xiao Y, Zhang X, Duan HC, Jia G. 2018. The m(6)A Reader ECT2 Controls Trichome Morphology by Affecting mRNA Stability in Arabidopsis. *Plant Cell* **30**(5): 968-985.

Wickham H, Wickham H. 2016. *Data analysis*: Springer.

Wu H, Ma T, Kang M, Ai F, Zhang J, Dong G, Liu J. 2019. A high-quality *Actinidia chinensis* (kiwifruit) genome. *Horticulture Research* **6**(1): 117.

Wu T, Hu E, Xu S, Chen M, Guo P, Dai Z, Feng T, Zhou L, Tang W, Zhan L, et al. 2021. clusterProfiler 4.0: A universal enrichment tool for interpreting omics data. *The Innovation* **2**(3): 100141.

Xiang S, Yan Z, Liu K, Zhang Y, Sun Z. 2016. AthMethPre: a web server for the prediction and query of mRNA m(6)A sites in Arabidopsis thaliana. *Molecular bioSystems* **12**(11): 3333-3337.

Yin X-r, Allan AC, Chen K-s, Ferguson IB. 2010. Kiwifruit EIL and ERF Genes Involved in Regulating Fruit Ripening. *Plant Physiology* **153**(3): 1280-1292.

Yu G, Wang L-G, Han Y, He Q-YJOajoib. 2012. clusterProfiler: an R package for comparing biological themes among gene clusters. *Omics: a journal of integrative biology* **16**(5): 284-287.

Yue H, Nie X, Yan Z, Weining S. 2019. N6-methyladenosine regulatory machinery in plants: composition, function and evolution. *Plant Biotechnology Journal* **17**(7): 1194-1208.

Zhang TY, Wang ZQ, Hu HC, Chen ZQ, Liu P, Gao SQ, Zhang F, He L, Jin P, Xu MZ, et al. 2021. Transcriptome-Wide N(6)-Methyladenosine (m(6)A) Profiling of Susceptible and Resistant Wheat Varieties Reveals the Involvement of Variety-Specific m(6)A Modification Involved in Virus-Host Interaction Pathways. *Frontiers in Microbiology* **12**: 656302.

Zhang Y, Liu T, Meyer CA, Eeckhoute J, Johnson DS, Bernstein BE, Nusbaum C, Myers RM, Brown M, Li W, et al. 2008. Model-based analysis of ChIP-Seq (MACS). *Genome Biology* **9**(9): R137.

Zheng H, Li S, Zhang X, Sui N. 2020. Functional Implications of Active N(6)-Methyladenosine in Plants. *Frontiers in Cell and Developmental Biology* **8**: 291.

Zhong S, Li H, Bodi Z, Button J, Vespa L, Herzog M, Fray RG. 2008. MTA is an Arabidopsis messenger RNA adenosine methylase and interacts with a homolog of a sex-specific splicing factor. *Plant Cell* **20**(5): 1278-1288.

Zhou L, Tang R, Li X, Tian S, Li B, Qin G. 2021. N6-methyladenosine RNA modification regulates strawberry fruit ripening in an ABA-dependent manner. *Genome Biology* **22**(1): 168.

Zhou L, Tian S, Qin G. 2019. RNA methylomes reveal the m6A-mediated regulation of DNA demethylase gene SlDML2 in tomato fruit ripening. *Genome Biology* **20**(1): 156.

Figure Legends

Fig. 1 m6A exhibits widespread presence during kiwifruit ripening. (a) Phenotypic alterations observed in kiwifruit (Actinidia chinensis cv. *Hongyang*) across four distinct stages of fruit development and ripening. (b) The alterations in ethylene levels in kiwifruit subsequent to the harvest at 185 DAP were examined. (c) Venn diagram was constructed to illustrate the concurrence of m6A peaks identified in two distinct m6A-seq experiments conducted on kiwifruit across four distinct development and ripening stages. (d) The bar graph displays the count of m6A peaks within transcripts at various time intervals during the various kiwifruit ripening stage. (e) LC-MS/MS assay revealed the levels of mRNA m6A in kiwifruits at four different stages. Data are presented as mean ± standard deviation (n = 3). Asterisks indicate statistical significance using Student's ***t***-test: *, $P < 0.05$.

Fig. 2 Alterations in m6A abundance during kiwifruit development and ripening. (a) Distribution of m6A modifications in kiwifruit across four development and ripening stages exhibited predominant enrichment in the vicinity of the stop codon and within the 3' UTR. (b) The distribution of m6A absolute enrichment across distinct genomic regions was examined at four successive development and ripening stages of kiwifruit. (c) The distribution of m6A relative enrichment across distinct genomic regions was examined at four successive development and ripening stages of kiwifruit. (d) Sequence motifs within m6A peaks were detected utilizing the HOMER.

Fig. 3 Impact of m6A modification on mRNA transcriptional levels in kiwifruit at distinct development and ripening stages. (a) Construct scatter plots to visualize the changes in expression levels of 913 upregulated hypermethylated transcripts at 160 days after pollination (DAP) and 1004 upregulated hypermethylated transcripts at 185 DAP, particularly observed in kiwifruit samples collected at 160 DAP and 185 days, respectively. (b) Scatter plots depict the variations in expression levels of 1444 upregulated hypermethylated transcripts at 185 DAP and 891 upregulated hypermethylated transcripts at 185 DAP + 5, specifically in kiwifruit samples collected at 185 DAP and 185 DAP + 5, respectively. (c) Gene expression ratios and box plots reveal the methylated distribution of mRNA abundance in kiwifruit at 185 DAP in comparison to kiwifruit at 160 DAP. (d) Gene expression ratios and box plots demonstrate the methylated distribution of mRNA abundance in kiwifruit at 185 DAP + 5 compared to kiwifruit at 185 DAP. (e) and (f) respectively represent genes with distinct m6A peaks in each region during the development stages at 185 days after pollination (DAP) and 185 DAP + 5, along with their corresponding expression levels.

Fig. 4 m6A modification level of fruit ripening-related genes and its expression changes affect kiwifruit ripening. (a), (b) The mRNA levels of ethylene receptor-like proteins

Acc27491 and Acc04179 and the levels of m6A immunoprecipitation combined with qPCR (m6A-IP-qPCR) in kiwifruit at different development and ripening stages. (c), (d) The mRNA levels and m6A immunoprecipitation combined qPCR (m6A-IP-qPCR) levels of sucrose accumulation-related genes *Acc23267* and *Acc25497* in kiwifruit at different development and ripening stages. *ACTIN* was used to normalize the expression values. The error bars represent the standard deviation of three independent experiments.

Fig. 5 Impact of AcALKBH10 and AcECT9 on the ripening characteristics of kiwifruit. (a) The expression patterns of relevant epigenetic writer, reader, and eraser proteins in kiwifruit at various development stages were analyzed using RNA-seq data obtained from previous studies conducted by Wang *et al.* (2022) and Shu *et al*. (2023). (b) The expression level of *AcALKBH10* after transient overexpression and silencing in kiwifruit at 120 DAP. (c) The present study entails the determination outcomes of sugars and acids composition of metabolites in kiwifruit plant samples pertaining to two distinct genetic modifications, namely the overexpression lines of *AcALKH10* and the silent lines. (d) Expression levels of fruit ripening-related genes in kiwifruit *AcALKH10* overexpression lines and silent lines. (e) The expression level of *AcECT9* after transient overexpression and silencing in kiwifruit at 120 DAP. (f) The present study entails the determination outcomes of sugars and acids composition of metabolites in kiwifruit plant samples pertaining to two distinct genetic modifications, namely the overexpression lines of *AcECT9* and the silent lines. (g) Expression levels of fruit ripening-related genes in kiwifruit *AcECT9* overexpression lines and silent lines. Asterisks indicate statistical significance using Student's ***t***-test: *, $P < 0.05$.

Fig. 6 Impact of exogenous AcALKBH10 expression on tomato fruit ripening. (a) Distinct stages of maturation in wild-type (WT) and *AcALKBH10* overexpression (*AcALKBH10*-OE) lines were observed. The overexpression line exhibited an accelerated ripening phenotype in its fruits. (b) The sugar and acid composition in fruits of both WT and *AcALKBH10*-OE lines were assessed at the Br+7 stage. The overexpression lines exhibited elevated sugar content and decreased acid content compared to the wild-type. Each line was evaluated using three independent biological replicates. (c), (d), and (e) correspondingly denote the relative transcript abundances of ripening-associated genes in tomato fruits at three distinct development stages, namely 36 days post-anthesis (DPA), Br+3 stage, and 42 DPA. Asterisks indicate statistical significance using Student's ***t***-test: *, $P < 0.05$.

Supporting Information

Supplemental Data 1 List of primers used in this study.

Supplemental Data 2 The sequencing quality of the kiwifruit MeRIP samples.

Supplemental Data 3 The m6A-seq experiment identified reliable m6A peaks in kiwifruit at different stages.

Supplemental Data 4 Gene expression profiles in kiwifruit at different stages.

Supplemental Data 5 The m6A density in actively expressed transcripts.

Supplemental Data 6 KEGG enrichment results for m6A-modificated genes in kiwifruit at different stages.

Supplemental Data 7 Transcripts with higher enrichment of m6A peaks were observed in kiwifruit at different ripening stages.

Supplemental Data 8 Transcripts of m6A-related proteins in kiwifruit at different stages of ripening.

Fig. S1 Pearson Correlation Coefficients (PCC) analysis of MeRIP sequencing at four development and ripening stages.

Fig. S2 Expression of key genes in ethylene biosynthesis.

Fig. S3 KEGG enrichment analysis on the actively expressed transcripts with m6A modification.

Fig. S4 Sequence motifs identified within m6A peaks using HOMER.

Fig. S5 Volcano plots were used to analyze the differences of m6A modification on transcripts during the kiwifruit ripening.

Fig. S6 Changes in kiwifruit mRNA transcription levels between 120 DAP and 160 DAP under varying abundances of m6A modifications.

Fig. S7 The m6A modification levels negatively regulate the expression of ripening-associated genes in kiwifruit.

Fig. S8 Phylogenetic analysis of the kiwifruit m6A modification related protein family.

Fig. S9 The impact of heterologous expression of *AcALKBH10* on the ripening process of tomato fruits.

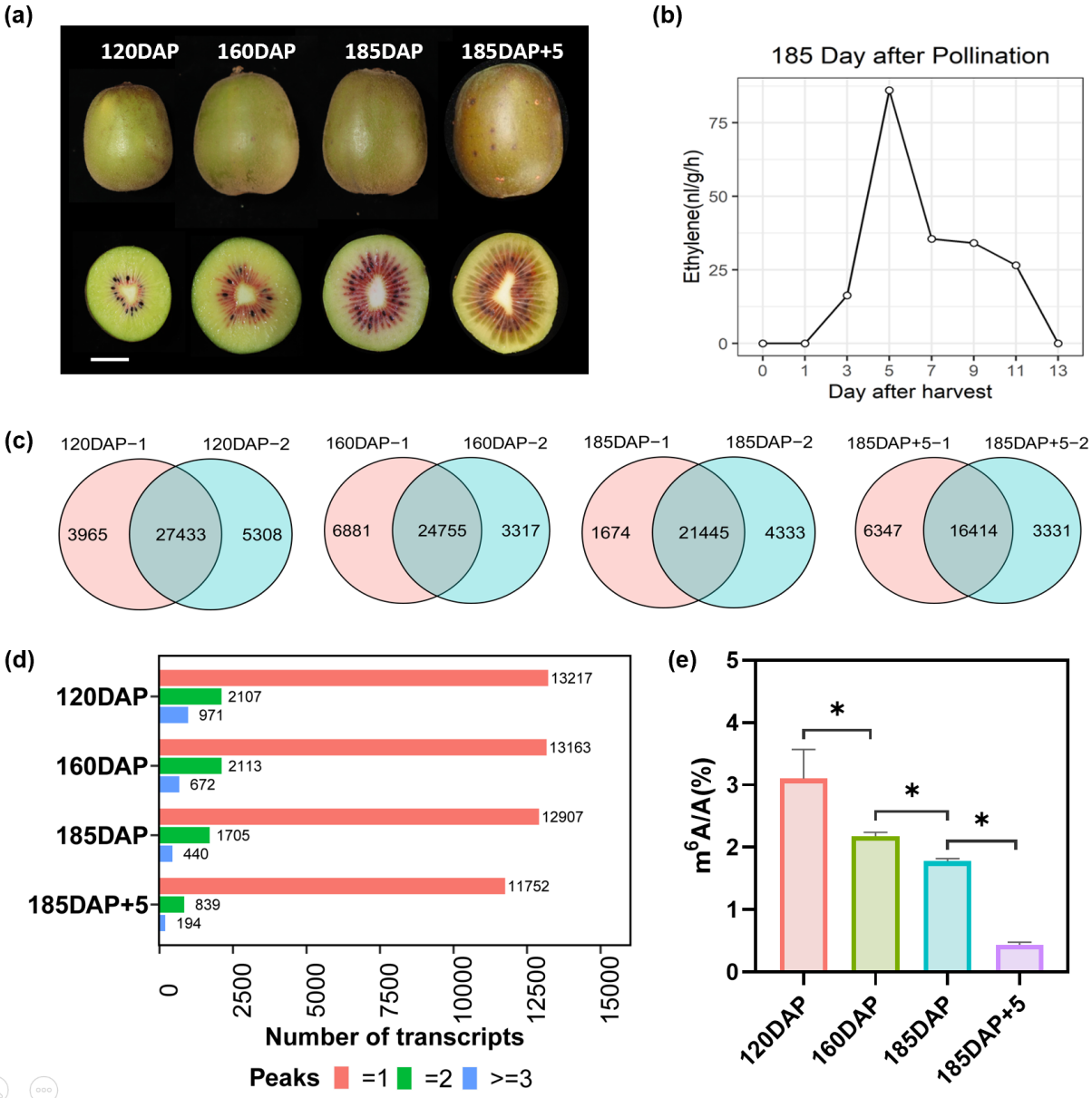
(a)
120DAP
160DAP
185DAP
185DAP+5
(b)
185 Day after Pollination
Ethylene(nl/g/h)
0
25
50
75
0 1 3 5 7 9 11 13
Day after harvest
(c)
120DAP−1
120DAP−2
3965
27433
5308
160DAP−1
160DAP−2
6881
24755
3317
185DAP−1
185DAP−2
1674
21445
4333
185DAP+5−1
185DAP+5−2
6347
16414
3331
(d)
120DAP
160DAP
185DAP
185DAP+5
13217
2107
971
13163
2113
672
12907
1705
440
11752
839
194
0
2500
5000
7500
10000
12500
15000
Number of transcripts
Peaks =1 =2 >=3
(e)
m6A/A(%)
0
1
2
3
4
5
*
*
*
120DAP
160DAP
185DAP
185DAP+5

Fig. 1 m6A exhibits widespread presence during kiwifruit ripening. (a) Phenotypic alterations observed in kiwifruit (Actinidia chinensis cv. *Hongyang*) across four distinct stages of fruit development and ripening. (b) The alterations in ethylene levels in kiwifruit subsequent to the harvest at 185 DAP were examined. (c) Venn diagram was constructed to illustrate the concurrence of m6A peaks identified in two distinct m6A-seq experiments conducted on kiwifruit across four distinct developmental and ripening stages. (d) The bar graph displays the count of m6A peaks within transcripts at various time intervals during the various kiwifruit ripening stage. (e) LC-MS/MS assay revealed the levels of mRNA m6A in kiwifruits at four different stages. Data are presented as mean ± standard deviation (n = 3). Asterisks indicate statistical significance using Student's ***t***-test: *, $P < 0.05$.

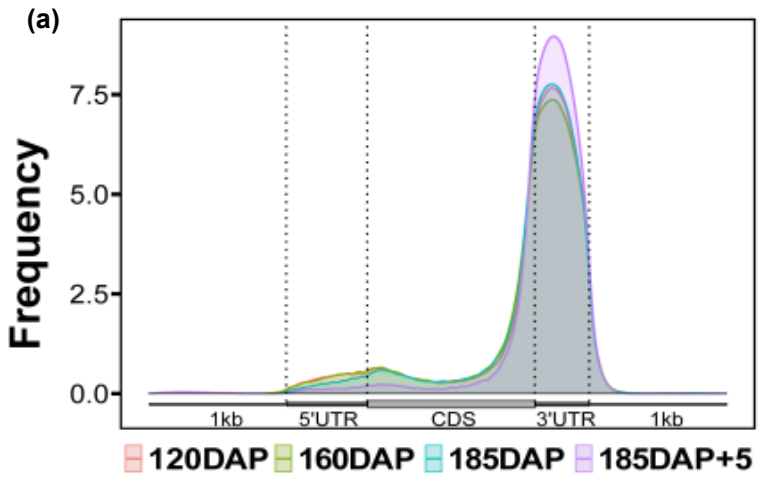
(a)
Frequency
7.5
5.0
2.5
0.0
1kb
5'UTR
CDS
3'UTR
1kb
120DAP
160DAP
185DAP
185DAP+5

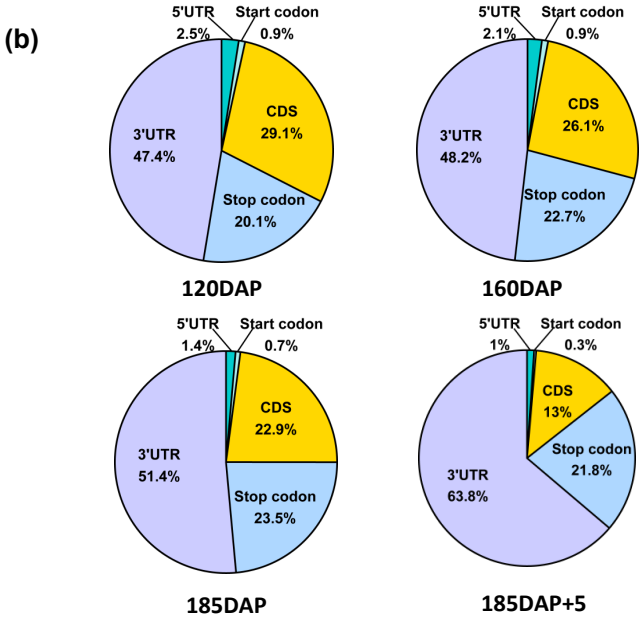
(b)
5'UTR 2.5%
Start codon 0.9%
CDS 29.1%
3'UTR 47.4%
Stop codon 20.1%
120DAP
5'UTR 2.1%
Start codon 0.9%
CDS 26.1%
3'UTR 48.2%
Stop codon 22.7%
160DAP
5'UTR 1.4%
Start codon 0.7%
CDS 22.9%
3'UTR 51.4%
Stop codon 23.5%
185DAP
5'UTR 1%
Start codon 0.3%
CDS 13%
Stop codon 21.8%
3'UTR 63.8%
185DAP+5

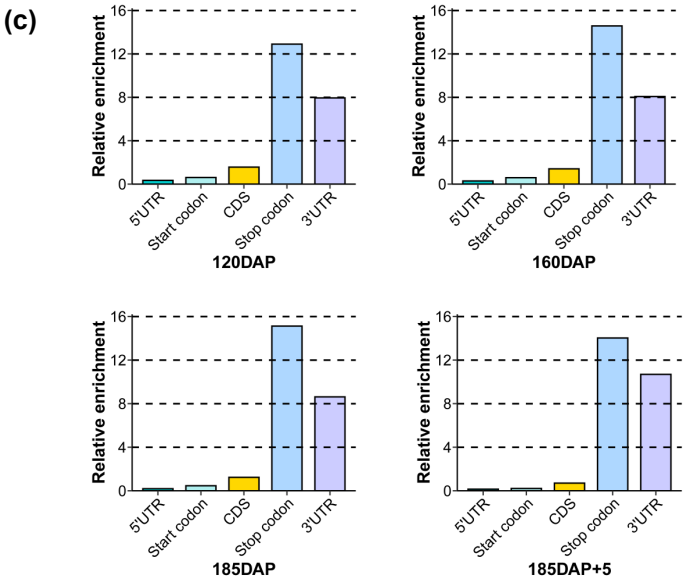
(c)
Relative enrichment
16
12
8
4
0
5'UTR
Start codon
CDS
Stop codon
3'UTR
120DAP
160DAP
185DAP
185DAP+5

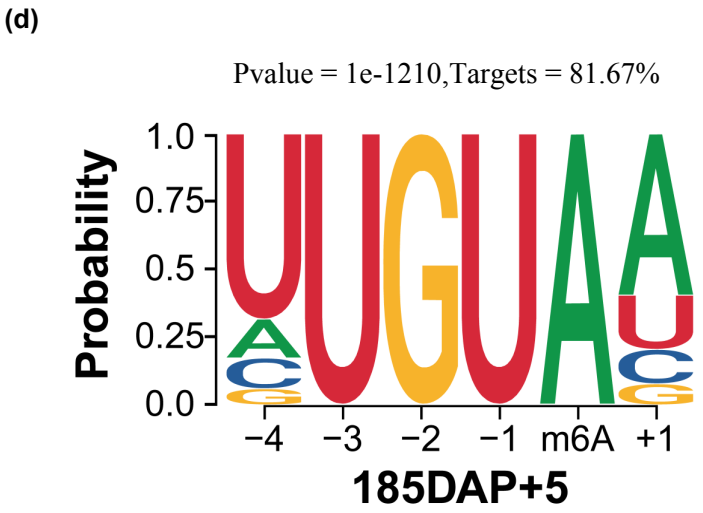
(d)
Pvalue = 1e-1210,Targets = 81.67%
Probability
1.0
0.75
0.5
0.25
0.0
−4
−3
−2
−1
m6A
+1
185DAP+5

Fig. 2 Alterations in m6A abundance during kiwifruit developmental and ripening. (a) Distribution of m6A modifications in kiwifruit across four developmental and ripening stages exhibited predominant enrichment in the vicinity of the stop codon and within the 3' UTR. (b) The distribution of m6A absolute enrichment across distinct genomic regions was examined at four successive developmental and ripening stages of kiwifruit. (c) The distribution of m6A relative enrichment across distinct genomic regions was examined at four successive developmental and ripening stages of kiwifruit. (d) Sequence motifs within m6A peaks were detected utilizing the HOMER.

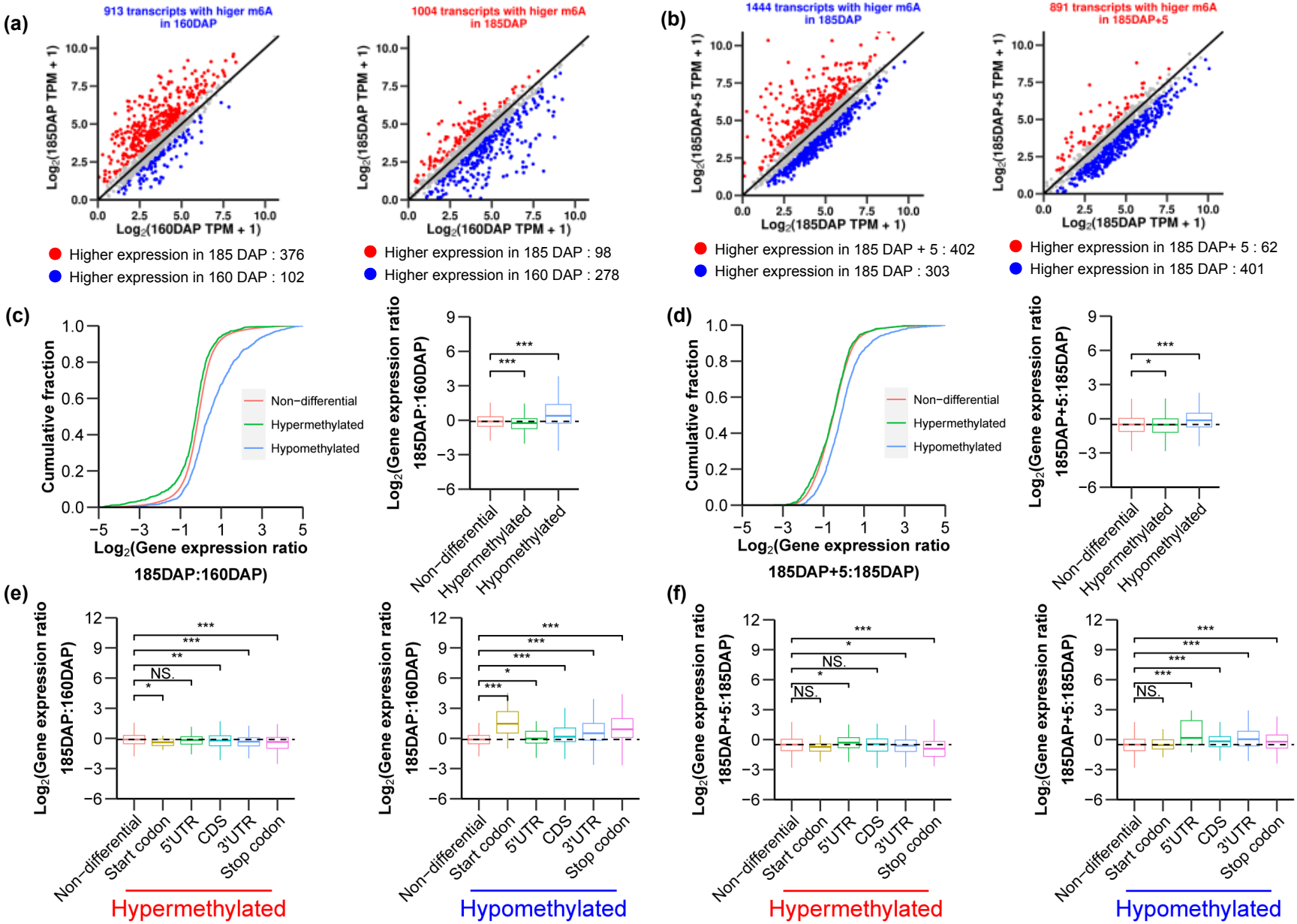
(a)
913 transcripts with higer m6A in 160DAP
Log2(185DAP TPM + 1)
Log2(160DAP TPM + 1)
Higher expression in 185 DAP : 376
Higher expression in 160 DAP : 102
1004 transcripts with higer m6A in 185DAP
Higher expression in 185 DAP : 98
Higher expression in 160 DAP : 278
(b)
1444 transcripts with higer m6A in 185DAP
Log2(185DAP+5 TPM + 1)
Log2(185DAP TPM + 1)
Higher expression in 185 DAP + 5 : 402
Higher expression in 185 DAP : 303
891 transcripts with higer m6A in 185DAP+5
Higher expression in 185 DAP+ 5 : 62
Higher expression in 185 DAP : 401
(c)
Cumulative fraction
Log2(Gene expression ratio 185DAP:160DAP)
Non−differential
Hypermethylated
Hypomethylated
Log2(Gene expression ratio 185DAP:160DAP)
(d)
Log2(Gene expression ratio 185DAP+5:185DAP)
(e)
Non−differential
Start codon
5'UTR
CDS
3'UTR
Stop codon
Hypermethylated
Hypomethylated
(f)

Fig. 3 Impact of m6A modification on mRNA transcriptional levels in kiwifruit at distinct developmental and ripening stages. (a) Construct scatter plots to visualize the changes in expression levels of 913 upregulated hypermethylated transcripts at 160 days after pollination (DAP) and 1004 upregulated hypermethylated transcripts at 185 DAP, particularly observed in kiwifruit samples collected at 160 DAP and 185 days, respectively. (b) Scatter plots depict the variations in expression levels of 1444 upregulated hypermethylated transcripts at 185 DAP and 891 upregulated hypermethylated transcripts at 185 DAP + 5, specifically in kiwifruit samples collected at 185 DAP and 185 DAP + 5, respectively. (c) Gene expression ratios and box plots reveal the methylated distribution of mRNA abundance in kiwifruit at 185 DAP in comparison to kiwifruit at 160 DAP. (d) Gene expression ratios and box plots demonstrate the methylated distribution of mRNA abundance in kiwifruit at 185 DAP + 5 compared to kiwifruit at 185 DAP. (e) and (f) respectively represent genes with distinct m6A peaks in each region during the developmental stages at 185 days after pollination (DAP) and 185 DAP + 5, along with their corresponding expression levels.

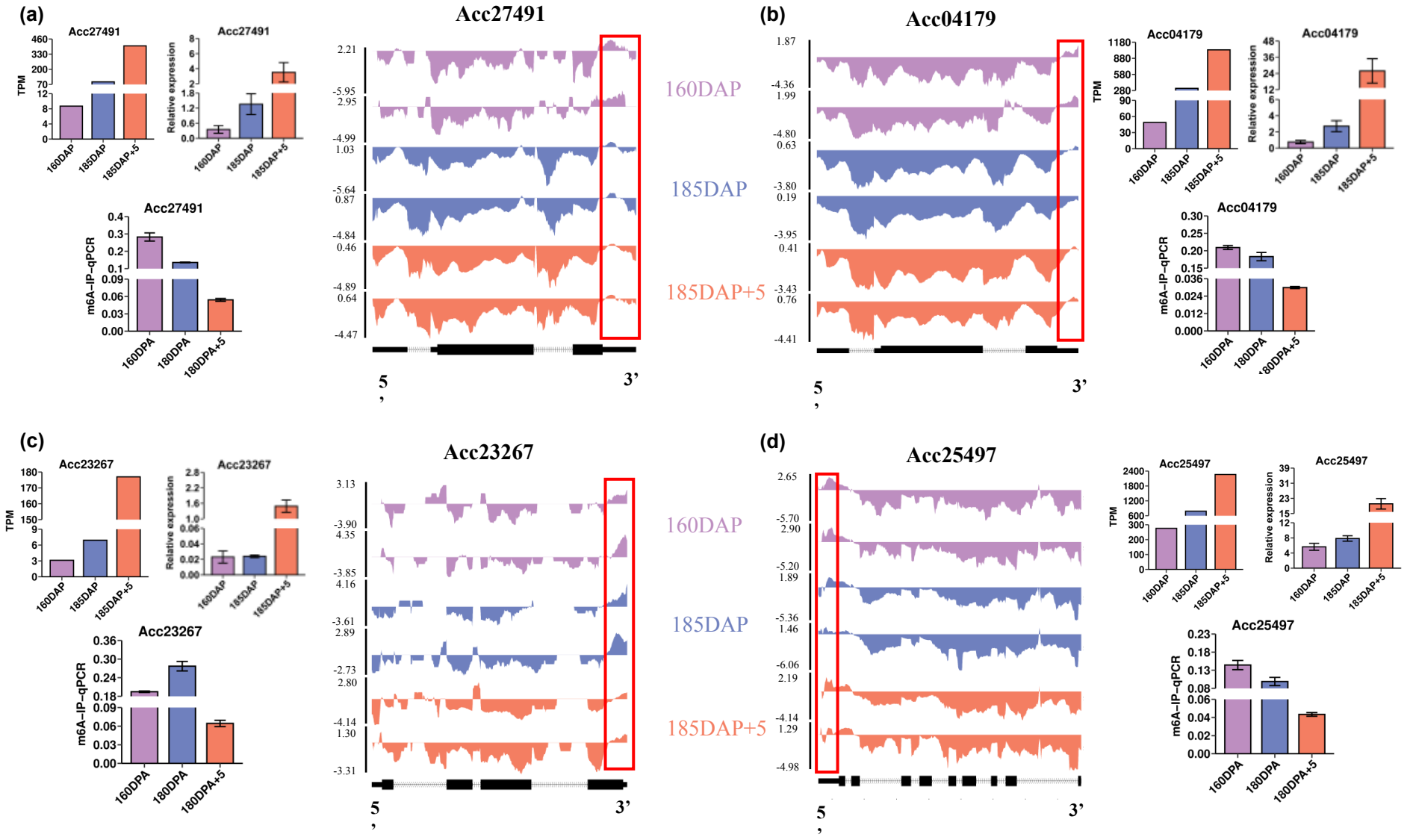
(a)
Acc27491
TPM
160DAP
185DAP
185DAP+5
Relative expression
m6A-IP-qPCR
160DPA
180DPA
180DPA+5
160DAP
185DAP
185DAP+5
5'
3'
(b)
Acc04179
(c)
Acc23267
(d)
Acc25497

Fig. 4 m6A modification level of fruit ripening-related genes and its expression changes affect kiwifruit ripening. (a), (b) The mRNA levels of ethylene receptor-like proteins Acc27491 and Acc04179 and the levels of m6A immunoprecipitation combined with qPCR (m6A-IP-qPCR) in kiwifruit at different developmental and ripening stages. (c), (d) The mRNA levels and m6A immunoprecipitation combined qPCR (m6A-IP-qPCR) levels of sucrose accumulation-related genes *Acc23267* and *Acc25497* in kiwifruit at different developmental and ripening stages. *ACTIN* was used to normalize the expression values. The error bars represent the standard deviation of three independent experiments.

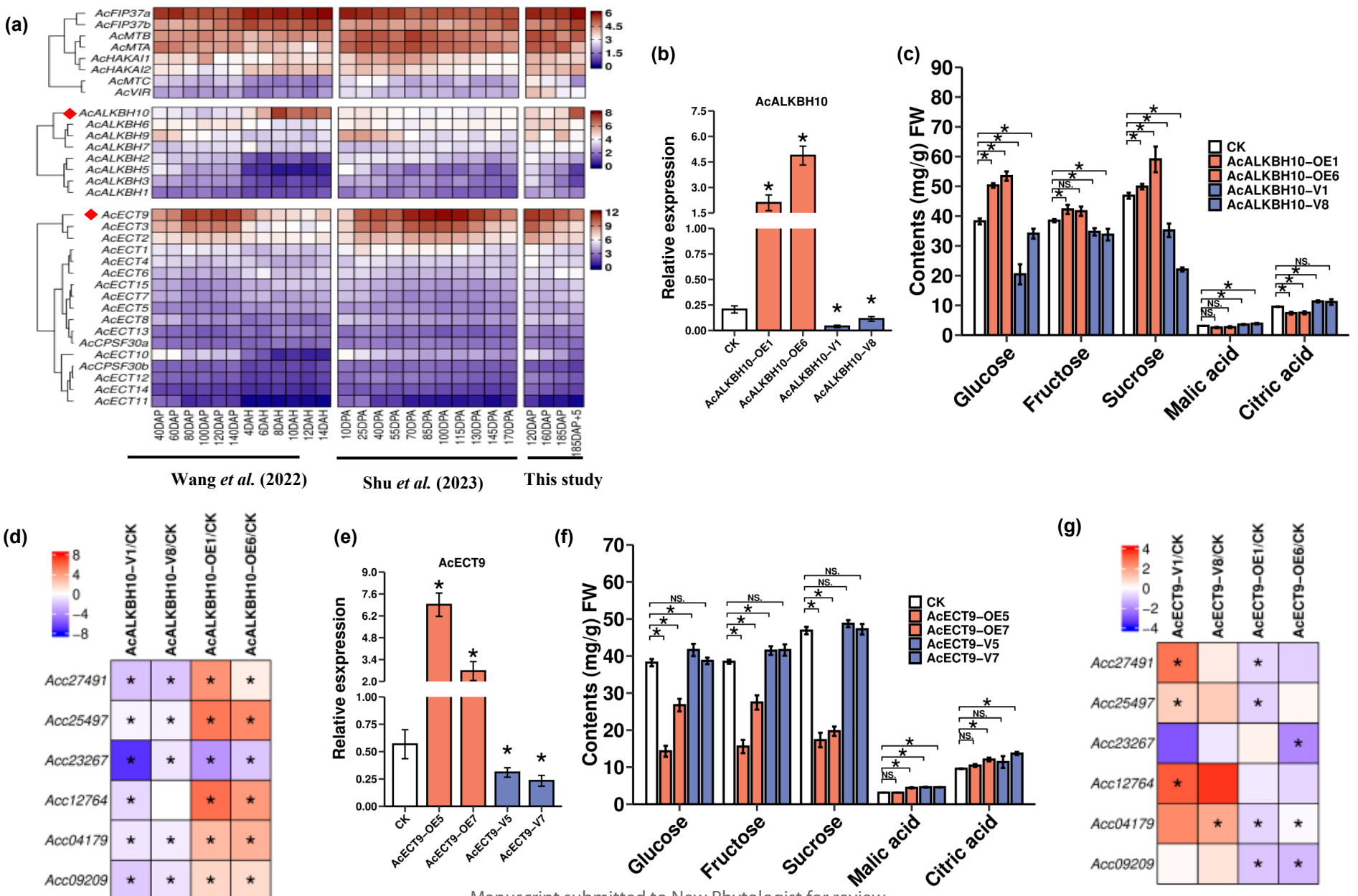
(a)
AcFIP37a
AcFIP37b
AcMTB
AcMTA
AcHAKAI1
AcHAKAI2
AcMTC
AcVIR
AcALKBH10
AcALKBH6
AcALKBH9
AcALKBH7
AcALKBH2
AcALKBH5
AcALKBH3
AcALKBH1
AcECT9
AcECT3
AcECT2
AcECT1
AcECT4
AcECT6
AcECT15
AcECT7
AcECT5
AcECT8
AcECT13
AcCPSF30a
AcECT10
AcCPSF30b
AcECT12
AcECT14
AcECT11
40DAP 60DAP 80DAP 100DAP 120DAP 140DAP 4DAH 6DAH 8DAH 10DAH 12DAH 14DAH
10DPA 25DPA 40DPA 55DPA 70DPA 85DPA 100DPA 115DPA 130DPA 145DPA 170DPA
120DAP 160DAP 185DAP 185DAP+5
Wang et al. (2022)
Shu et al. (2023)
This study
(b)
AcALKBH10
Relative esxpression
CK
AcALKBH10–OE1
AcALKBH10–OE6
AcALKBH10–V1
AcALKBH10–V8
(c)
Contents (mg/g) FW
CK
AcALKBH10–OE1
AcALKBH10–OE6
AcALKBH10–V1
AcALKBH10–V8
Glucose
Fructose
Sucrose
Malic acid
Citric acid
(d)
AcALKBH10–V1/CK
AcALKBH10–V8/CK
AcALKBH10–OE1/CK
AcALKBH10–OE6/CK
Acc27491
Acc25497
Acc23267
Acc12764
Acc04179
Acc09209
(e)
AcECT9
Relative esxpression
CK
AcECT9–OE5
AcECT9–OE7
AcECT9–V5
AcECT9–V7
(f)
Contents (mg/g) FW
CK
AcECT9–OE5
AcECT9–OE7
AcECT9–V5
AcECT9–V7
Glucose
Fructose
Sucrose
Malic acid
Citric acid
(g)
AcECT9–V1/CK
AcECT9–V8/CK
AcECT9–OE1/CK
AcECT9–OE6/CK
Acc27491
Acc25497
Acc23267
Acc12764
Acc04179
Acc09209

Fig. 5 Impact of AcALKBH10 and AcECT9 on the ripening characteristics of kiwifruit. (a) The expression patterns of relevant epigenetic writer, reader, and eraser proteins in kiwifruit at various developmental stages were analyzed using RNA-seq data obtained from previous studies conducted by Wang *et al.* (2022) and Shu *et al.* (2023). (b) The expression level of *AcALKBH10* after transient overexpression and silencing in kiwifruit at 120 DAP. (c) The present study entails the determination outcomes of sugars and acids composition of metabolites in kiwifruit plant samples pertaining to two distinct genetic modifications, namely the overexpression lines of *AcALKH10* and the silent lines. (d) Expression levels of fruit ripening-related genes in kiwifruit *AcALKH10* overexpression lines and silent lines. (e) The expression level of *AcECT9* after transient overexpression and silencing in kiwifruit at 120 DAP. (f) The present study entails the determination outcomes of sugars and acids composition of metabolites in kiwifruit plant samples pertaining to two distinct genetic modifications, namely the overexpression lines of *AcECT9* and the silent lines. (g) Expression levels of fruit ripening-related genes in kiwifruit *AcECT9* overexpression lines and silent lines. Asterisks indicate statistical significance using Student's ***t***-test: *, $P < 0.05$.

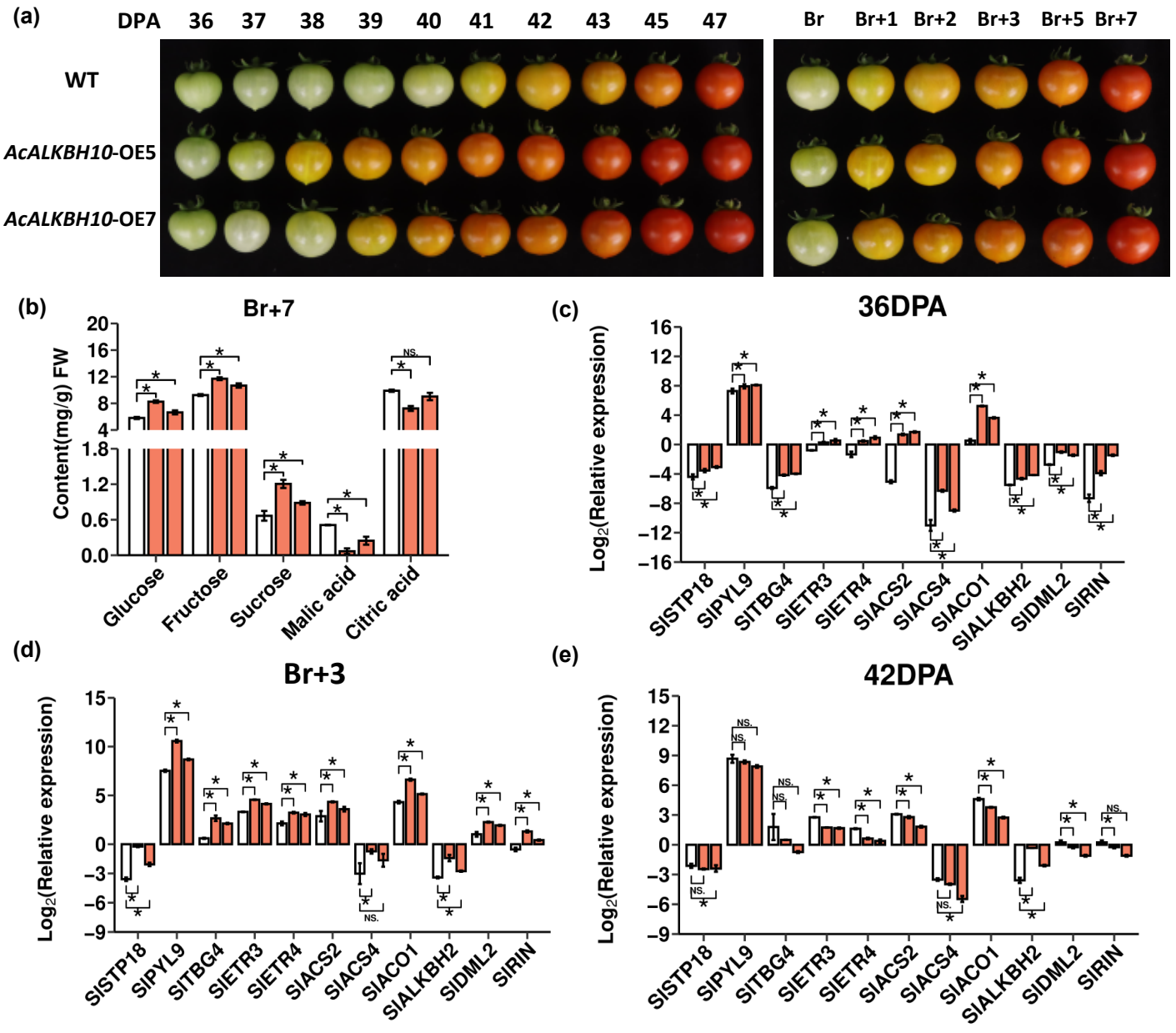
(a)
DPA 36 37 38 39 40 41 42 43 45 47
Br Br+1 Br+2 Br+3 Br+5 Br+7
WT
AcALKBH10-OE5
AcALKBH10-OE7
(b)
Br+7
Content(mg/g) FW
Glucose
Fructose
Sucrose
Malic acid
Citric acid
(c)
36DPA
Log2(Relative expression)
(d)
Br+3
(e)
42DPA
SlSTP18 SlPYL9 SlTBG4 SlETR3 SlETR4 SlACS2 SlACS4 SlACO1 SlALKBH2 SlDML2 SlRIN
WT AcALKBH10-OE5 AcALKBH10-OE7

Fig. 6 Impact of exogenous *AcALKBH10* expression on tomato fruit ripening. (a) Distinct stages of maturation in wild-type (WT) and *AcALKBH10* overexpression (*AcALKBH10*-OE) lines were observed. The overexpression line exhibited an accelerated ripening phenotype in its fruits. (b) The sugar and acid composition in fruits of both WT and *AcALKBH10*-OE lines were assessed at the Br+7 stage. The overexpression lines exhibited elevated sugar content and decreased acid content compared to the wild-type. Each line was evaluated using three independent biological replicates. (c), (d), and (e) correspondingly denote the relative transcript abundances of ripening-associated genes in tomato fruits at three distinct developmental stages, namely 36 days post-anthesis (DPA), Br+3 stage, and 42 DPA. Asterisks indicate statistical significance using Student's ***t***-test: *, $P < 0.05$.